SLAC-PUB-4877
March 1989
T/E

PRODUCTION OF NEUTRAL BOSONS BY AN ELECTRON BEAM*

YUNG SU TSAI

Stanford Linear Accelerator Center
Stanford University, Stanford, California 94309

ABSTRACT

We investigate the possible existence of neutral bosons which are coupled to leptons. The cross section for the process $e + p \to e + X +$ anything, where X is a neutral boson of spin-parity $0^{\pm}$ or $1^{\pm}$ emitted by the electron, is calculated and its energy-angle distribution discussed. Assuming X to decay predominantly into a lepton pair we investigate the characteristics of the background. It is pointed out that the signal to the background ratio can be greatly enhanced if one selects high $x = E_x/E_1$ and also uses the outgoing electron as a tag at a slightly non-forward angle with the X particle arranged in such a way that the momentum transfer to the target particle is near its minimum. This happens when the outgoing electron momentum $\vec{P}_2$ is parallel to $\vec{P}_1 - \vec{k}$, where $\vec{P}_1$ and $\vec{k}$ are the momenta of the incident electron and the X particle respectively.

Submitted to *Physical Review D*

⋆ Work supported by the Department of Energy, contract DE–AC03–76SF00515.

I. INTRODUCTION

In gauge theories with spontaneously broken symmetry, bosons with spin-parity $0^\pm$ and $1^\pm$ play very essential roles. Up to now the standard theory of SU3 $\times$ SU2 $\times$ U(1) worked rather well, but one is never sure that there might not be some unexpected particles to be discovered. The existence of unexpected vector or scalar (or pseudo scalar) particles would certainly change our concept of the elementary particle world as we understand it today. The purpose of this paper is to investigate the feasibility of producing such particles using the electron beams at SLAC. While these beams have only modest energies, their high intensities permit searches for bosons that might be very weakly coupled to electrons. We denote the particle we are looking for as X which can be a vector, axial vector, scalar or pseudoscalar particle. Since we hope to produce it by an electron via bremsstrahlung we assume that the X particle is coupled to an electron with a coupling constant g_x:

$$\begin{array}{rl} g_x \; x \; \overline{u}\,(P_2)\; u\,(P_1) & \text{if } X \text{ is a scalar,} \\ g_x \; x \; \overline{u}\,(P_2)\; \gamma_5 \; u\,(P_1) & \text{if } X \text{ is a pseudo scalar,} \\ g_x \; x_\mu \; \overline{u}\,(P_2)\; \gamma^\mu \; u\,(P_1) & \text{if } X \text{ is a vector,} \\ g_x \; x_\mu \; \overline{u}\,(P_2)\; \gamma_5 \; \gamma^\mu \; u\,(P_1) & \text{if } X \text{ is an axial vector.} \end{array}$$

We define $\alpha_x \equiv g_x^2/(4\pi)$.

The mechanism of production of the X particle is shown in Fig. 1. P_1 and P_2 represent the four momenta of the incident and outgoing electrons, k is the four momentum of the X particle. P_i and P_f are four momenta of the initial and final target particles, respectively. In this paper the target particle is a proton from a hydrogen jet injected into the PEP ring and P_1 is the 14.5 GeV circulating electron beam as suggested in the PEGASYS proposal[1] at SLAC. Our calculations can be adapted to a stationary target using a heavier element or the e^+ target in the e^+e^- colliding beam. Only the change in target form factors is required for the adaptation. The X particle is detected through its decay into e^+e^- or $\mu^+\mu^-$ pair.

A similar calculation[2] was done previously by this author for production of a 1.7 MeV object using the Weizsacker–Williams method. The subsequent searches by Riordan[3] *et al.*, Konaka[4] *et al.*, Davier[5] *et al.*, and Brown[6] *et al.*, all showed that the 1.7 MeV object observed[7] at GSI could not be an elementary particle. These experiments gave also the upper limits of α_x as a function of m_x in the range 1 MeV $< m_x <$ 15 MeV. Another powerful constraint[8] on the value of α_x as a function of m_x is obtained by $g-2$ values of electron and muon. The most up-to-date discussions of the range of α_x and m_x ruled out by all these experiments, including $g-2$, beam dump and, $e^+e^- \to X \to e^+e^-$ are given by Hawkins and Perl.[9]

II. CALCULATIONS

The cross section for the process $e + P_i \to X + e + P_f$, shown in Fig. 1, can be written as

$$d\sigma = \frac{\alpha^2 \alpha_x}{2\pi^2 P_1} \int \frac{d^3k}{E_x} \int \frac{d^3P_2}{E_2} \, (F_{1i}W_1 + F_{2i}W_2)/t^2 \quad , \tag{2.1}$$

where k is the momentum of the produced X particle, t is the momentum transfer squared to the target, and W_1 and W_2 are the usual target form factors used in the electron scattering.[11] F_{1i} and F_{2i} represent the matrix elements squared for the emission of an X particle of kind i (scalar, pseudo scalar, vector and axial vector) and they are algebraically computed using a computer in the following way: We first define F_1 for production of an axial vector particle X:

$$\begin{aligned}F_{1av} = -\frac{T_r}{4}[(\not{P}_1 + m_e)\bigg\{&\frac{\gamma_\mu(\not{q} + \not{P}_1)\gamma_\nu\gamma_5 + \gamma_\mu\gamma_\nu\gamma_5 m_e}{2B} \\ &- \frac{\gamma_\nu\gamma_5(\not{P}_2 - \not{q})\gamma_\mu + \gamma_\nu\gamma_5\gamma_\mu m_e}{2C}\bigg\}(\not{P}_2 + m_e) \\ &\bigg\{\frac{\gamma_5\gamma_{\nu'}(\not{q} + \not{P}_1)\gamma_\mu + \gamma_5\gamma_{\nu'}\gamma_\mu m_e}{2B} \\ &- \frac{\gamma_\mu(\not{P}_2 - \not{q})\gamma_5\gamma_{\nu'} + \gamma_\mu\gamma_5\gamma_{\nu'} m_e}{2C}\bigg\}\left(\frac{k\nu k\nu'}{m_x^2} - g_{\nu\nu'}\right) \quad ,\end{aligned} \tag{2.2}$$

where $B = P_2 \cdot k + m_x^2/2$, $C = P_1 \cdot k - m_x^2/2$ and $q = P_i - P_f$. We then obtain F_{2av} by the substitution:

$$F_{2av} = -F_{1av}(\gamma_\mu \to \not{P}_i)/M_i^2 \quad . \tag{2.3}$$

All other F_{1i} and F_{2i} are obtained by the following sequence of substitutions:

$$F_{1v} = -F_{1av}\ (\gamma_5 \to 1) \quad , \tag{2.4}$$

$$F_{2v} = -F_{2av}\ (\gamma_5 \to 1) \quad , \tag{2.5}$$

$$F_{1ps} = F_{1av}\ (\gamma_\nu \to 1\ ,\ \gamma_{\nu'} \to 1 \quad ,\quad k\nu k\nu'/m_x^2 - g_{\nu\nu'} \to 1) \quad , \tag{2.6}$$

$$F_{2ps} = -F_{1ps}\ (\gamma_\mu \to \not{P}_i)/M_i^2 \quad , \tag{2.7}$$

$$F_{1s} = -F_{1ps}\ (\gamma_5 \to 1) \quad , \tag{2.8}$$

$$F_{2s} = -F_{2ps}\ (\gamma_5 \to 1) \quad . \tag{2.9}$$

The trace in Eq. (2.2), as well as the subsequent substitutions shown in Eqs. (2.3) through (2.9), are handled by Hearn's[10] Reduce II Program. We shall not give all the results here because it is much easier to obtain the result directly from the computer than copying the lengthy expression from this paper. As long as the mass of the X particle m_x is much greater than the electron mass m_e, m_e can be ignored in the calculation. In the limit $m_e = 0$, we have relatively simple results that we give here:

$$F_{1s} = F_{1ps} = BS_{11} + S_{12} + B^{-1}S_{13} + B^{-2}S_{14} \tag{2.10}$$

$$F_{2s} = F_{2ps} = BS_{21} + S_{22} + B^{-1}S_{23} + B^{-2}S_{24} \tag{2.11}$$

$$F_{1v} = F_{1av} = BV_{11} + V_{12} + B^{-1}V_{13} + B^{-2}V_{14} \tag{2.12}$$

$$F_{2v} = F_{2av} = BV_{21} + V_{22} + B^{-1}V_{23} + B^{-2}V_{24} \tag{2.13}$$

where

$$S_{11} = 1/C \tag{2.14}$$

$$S_{12} = -(2 + m_x^2/C + tm_x^2/4/C^2) \tag{2.15}$$

$$S_{13} = Ctm_x^2 + m_x^4/C/2 \tag{2.16}$$

$$S_{14} = -tm_x^2/4 \tag{2.17}$$

$$S_{21} = -1/(2C) \tag{2.18}$$

$$S_{22} = 1 - (E_1E_x - E_2E_x - E_x^2)/C + (t/8 - E_1E_2/2 + E_2E_x/2)m_x^2/C^2 \tag{2.19}$$

$$S_{23} = -C/2 + E_1E_x - E_2E_x - E_x^2 - tm_x^2/(4C) + tE_x^2/(2C) \tag{2.20}$$

$$+ (E_1E_2 + E_1E_x/2 - E_2E_x/2 - E_x^2/2)m_x^2/C \tag{2.21}$$

$$S_{24} = (t - 4E_1E_2 - 4E_1E_x)m_x^2/8 \tag{2.22}$$

$$V_{11} = 2/C \tag{2.23}$$

$$V_{12} = 2t/C - 2m_x^2/C - tm_x^2/C^2/2 \tag{2.24}$$

$$V_{13} = 2C - 2t + 2m_x^2 + t^2/C - 2tm_x^2/C + m_x^4/C \tag{2.25}$$

$$V_{14} = -tm_x^2/2 \tag{2.26}$$

$$V_{21} = -1/C \tag{2.27}$$

$$V_{22} = (t - 2E_1^2 + 2E_1E_2 + 2E_1E_x)/C + (t/4 - E_1E_2 + E_2E_x)m_x^2/C^2 \tag{2.28}$$

$$\begin{aligned} V_{23} = {} & -C + t - 2E_1E_2 + 2E_2^2 + 2E_2E_x + (-t^2/2 + tm_x^2/2 + 2tE_1E_2 \\ & + tE_1E_x - tE_2E_x + m_x^2E_1^2 - m_x^2E_1E_x + m_x^2E_2^2 + m_x^2E_2E_x)/C \end{aligned} \tag{2.29}$$

$$V_{24} = (t/4 - E_1E_2 - E_1E_x)m_x^2 \tag{2.30}$$

In the above expressions $t = -(P_1 - P_2 - k)^2$, $B = P_2 \cdot k + m_x^2/2$, $C = P_1 \cdot k - m_x^2/2$, and E_1, E_2 and E_x are the laboratory energies of the incident and outgoing electrons and the X particle, respectively. They can be expressed covariantly as $E_1 = P_1 \cdot P_i/M_i$, $E_2 = P_2 \cdot P_i/M_i$ and $E_x = k \cdot P_i/M_i$ if one is interested in using our results in other coordinate systems. The target form factors W_1 and W_2 are functions of t and $M_f^2 = P_f^2$. The type of form factors to be used depends upon the magnitude of t. If $\sqrt{t}$ is comparable to the inverse of the atomic radius, i.e., $\sqrt{t} \sim 10eVZ^{1/3}$, then atomic form factors must be used. If $\sqrt{t}$ is comparable to the inverse of the nuclear radius, i.e., $\sqrt{t} \sim .4A^{-1/3}$ GeV, then nuclear form factors must be used. When $\sqrt{t}$ is comparable to the inverse of the proton radius then the nucleon form factors must be used. The computer can be programmed to select the proper form factors automatically according to the value of t. Comprehensive accounts of atomic form factors, nuclear form factors and nucleon form factors for dealing with this type of problem are given in Ref. 11. The reader should refer to that paper for details on W_1 and W_2 for various targets. The deep inelastic nucleon form factors given in that paper need to be up-dated.

The elastic form factors for a proton used in our calculations are:

$$\begin{bmatrix} W_{2p}^{el} \\ W_{1p}^{el} \end{bmatrix} = \frac{2M_p\delta(M_f^2 - M_p^2)}{(1+t/0.71)^4} \begin{bmatrix} (1+2.79^2\tau)/(1+\tau) \\ 2.79^2\tau \end{bmatrix} \quad , \tag{2.31}$$

where $\tau = t/(4M_p^2)$.

For the inelastic form factors for a proton[12] we use

$$W_{2p}^{ie} = (1-x')^3(.6453 + 1.902(1-x') - 2.343(1-x')^2)/\nu \tag{2.32}$$

$$W_{1p}^{ie} = 0.2W_{2p}^{ie} \quad , \tag{2.33}$$

where $x' = t/(t+M_f^2)$ and $\nu = (M_f^2 + t - M_p^2)/(2M_p)$.

Equation (2.1) can be used by the experimenters to estimate the number of X produced in their detector with α_x and m_x as free parameters. The Monte Carlo method is usually used for this purpose in order to accommodate various cuts and the detection efficiency, which must be folded into the integration of Eq. (2.1). Such detailed considerations are best left to the experimentalists.[13] In this paper, we investigate some essential features of the cross section and the backgrounds in order to aid experimentalists in designing their experiment. In order to do this, we integrate the cross section given by (2.1) with respect to d^3P_2, as well as the solid angle of the X particle, and obtain $d\sigma/dx$, where $x = E_x/E_1$. This will give us the order of magnitude of the production cross section and the energy distribution of the X particle. Since m_x and α_x are free parameters in the calculation, we shall be able to estimate the range of m_x and α_x for which an experiment is sensitive for a given integrated luminosity. We shall also discuss the energy-angle distribution $d\sigma/(dxd\theta)$ of the X particle. Finally, we shall show that the signal-to-noise ratio is increased by tagging the x production with the outgoing electron at high x and at angles such that $\overrightarrow{P_2}$ is parallel to $\overrightarrow{P_1} - \vec{k}$.

There are six-fold integrations in Eq. (2.1) if W_1 and W_2 represent inelastic form factors, but the number of integration is reduced by one if the final state has a discrete mass such as a proton. We perform the P_2 integration in the coordinate system where $u = P_2 + P_f = P_1 - k + P_i$ is at rest and $\vec{P}_1 - \vec{k}$ is in the z axis and both $\vec{k}$ and $\vec{P}_1$ are in the xz plane, as shown in Fig. 2. After integration with respect to P_2 in this special frame we do integration with respect to k in the laboratory system, with the direction of $\vec{P}_1$ as the z axis. The advantage of doing the P_2 integration in the special coordinate system is that only the quantity B in Eq. (2.1) depends upon, ϕ_2 and hence ϕ_2 integration can be carried out immediately.

$$
\begin{aligned}
B &= P_2 \cdot k + m_x^2/2 \\
&= E_{2s}E_{xs} - P_{2s}P_{xs}(\sin\theta_2 \sin\theta_k \cos\phi_2 + \cos\theta_2 \cos\theta_k) + m_x^2/2 \quad .
\end{aligned}
$$

Therefore

$$\frac{1}{2\pi}\int_0^{2\pi} B d\phi_2 = E_{2s}E_{xs} - P_{2s}P_{xs}\cos\theta_2\cos\theta_k + m_x^2/2 \equiv W \tag{2.34}$$

$$\frac{1}{2\pi}\int_0^{2\pi} \frac{1}{B} d\phi_2 = 1/SQRT(W^2 - P_{2s}^2 P_{xs}^2 \sin^2\theta_2 \sin^2\theta_k) \equiv Y^{-1} \tag{2.35}$$

$$\frac{1}{2\pi}\int_0^{2\pi} \frac{1}{B^2} d\phi_2 = W/Y^3 \tag{2.36}$$

Quantities with a subscript s refer to the rest frame of $u = P_2 + P_f$, and they can be expressed in terms of laboratory quantities in the following way:

$$C = P_1 \cdot k - m_x^2/2 = E_1(E_x - P_x \cos\theta) - m_x^2/2 \quad ,$$

where θ is the angle between the X particle and the incident electron in the laboratory system and $P_x = (E_x^2 - m_x^2)^{\frac{1}{2}}$ is the momentum of the X particle in the laboratory system.

$$
\begin{aligned}
U2 &\doteq (P_1+P_i-k)^2=(P_2+P_f)^2=M_p^2+2(E_1-E_x)M_p-2C \\
U &= SQRT(U2) \\
E_{xs} &= (C-m_x^2/2+E_xM_p)/U \\
P_{xs} &= SQRT(E_{xs}^2-m_x^2) \\
E_{2s} &= (U2-M_f^2)/2/U \\
E_{1s} &= (E_1M_p-C-m_x^2/2)/U \\
E_{is} &= M_p(E_1+M_p-E_x)/U \\
P_{is} &= SQRT(E_{is}^2-M_p^2) \\
\cos\theta_k &= [(E_{1s}-E_{xs})E_{xs}-C+m_x^2/2]/P_{xs}/P_{is} \\
E_2 &= (-M_p^2-t-M_f^2+2E_{is}U)/2/M_p \\
t &= 2C+2E_{2s}(E_{1s}-E_{xs})-2E_{2s}P_{is}\cos\theta_2
\end{aligned}
\tag{2.38}
$$

The integrations with respect to E_{2s} and $\cos\theta_2$ can be converted into integrations with respect to M_f^2 and t, respectively, using (2.37) and (2.38). We obtain from (2.1):

$$
\frac{d\sigma}{dx}\equiv 2\alpha^2\alpha_x f(x) \quad , \tag{2.39}
$$

where $x=E_x/E_1$ and

$$
f(x)=\frac{P_x}{4}\int_0^{\theta_{max}}\sin\theta d\theta\int_{M_f^2\,min}^{M_f^2\,max}dM_f^2\int_{t\,min}^{t\,max}dt(\overline{F}_{1i}W_1+\overline{F}_{2i}W_2)/t^2 \quad .
$$

$\overline{F}_{1i}$ and $\overline{F}_{2i}$ are F_{1i} and F_{2i} given by Eqs. (2.10) through (2.13) with B, $1/B$ and $1/B^2$ replaced by W, Y^{-1} and W/Y^3 respectively as shown in Eqs. (2.34) through

(2.36):

$$\overline{F}_{1s} = \overline{F}_{1ps} = WS_{11} + S_{12} + Y^{-1}S_{13} + (W/Y^3)S_{14}$$

$$\overline{F}_{2s} = \overline{F}_{2ps} = WS_{21} + S_{22} + Y^{-1}S_{23} + (W/Y^3)S_{24}$$

$$\overline{F}_{1v} = \overline{F}_{1av} = WV_{11} + V_{12} + Y^{-1}V_{13} + (W/Y^3)V_{14}$$

$$\overline{F}_{2v} = \overline{F}_{2av} = WV_{21} + V_{22} + Y^{-1}V_{23} + (W/Y^3)V_{24}$$

where S_{ij} and V_{ij} are defined by Eqs. (2.14) through (2.30).

The lower and upper limits of integrations for t are obtained from Eq. (2.38):

$$t_{\substack{max \\ min}} = 2C + 2E_{2s}(E_{1s} - E_{xs}) \pm 2E_{2s}P_{is} \quad . \tag{2.40}$$

For the elastic form factors, the integration with respect to M_f^2 drops out because of the δ function in Eq. (2.31). For inelastic form factors, the lower limit of M_f is given by the pion threshold.

$$(M_f^2)_{min} = (M_p + .14)^2 \quad , \tag{2.41}$$

and the upper limit can be obtained from Eq. (2.37),

$$(M_f^2)_{max} = U2 \quad . \tag{2.42}$$

The maximum production angle for the X particle, θ_{max}, can be obtained in the following way:

$$U2 = (P_1 - k + P_i)^2 = M_p^2 + M_x^2 - 2M_p(E_1 - E_x) - 2E_1(E_x - P_x \cos\theta) \quad .$$

Hence

$$\cos\theta_{max} = [(U2)_{min} - M_p^2 - M_x^2 + 2M_p(E_1 - E_p) + 2E_1E_2]/(2E_1P_x) \quad .$$

Now

$$(U2)_{min} = (P_2 + P_f)^2_{min} = (M_f^2)_{min} = \begin{cases} M_p^2 \text{ for elastic, and} \\ (M_p + .14)^2 \text{ for inelastic} \end{cases} \quad . \tag{2.43}$$

Therefore

$$\theta_{max} = arc\cos\left(\frac{(M_f^2)_{min} - M_p^2 - m_x^2 - 2M_pE_1(1-x) + 2E_1^2x}{2E_1^2x(1 - m_x^2/x^2/E_1^2)^{0.5}}\right) \quad . \tag{2.44}$$

where $x = E_x/E_1$.

The allowed range of $x = E_x/E_1$ can be obtained in the following way:

$$E_x = k \cdot P_i/M_p = (E_{xcm}E_{icm} - P_{xcm}E_{icm}\cos\theta_{ikcm})/M_p$$

where the subscript CM refers to the center-of-mass system. Thus

$$(E_x)_{\substack{max \\ min}} = (E_{xcm}E_{icm} \pm P_{xcm}P_{icm})/M_p \quad ;$$

now

$$\begin{aligned} E_{icm} &= M_p(E_1 + M_p)/W \\ E_{xcm} &= (W^2 - M_f^2 + m_x^2)/(2W) \quad , \end{aligned} \tag{2.45}$$

where $W = SQRT(M_p^2 + 2E_1M_p)$ and M_f^2 in (2.45) must be $(M_f^2)_{min}$ given by (2.43).

We conclude

$$X_{\substack{max \\ min}} = (E_{xcm}E_{icm} \pm P_{xcm}P_{icm})/M_p/E_1 \tag{2.46}$$

with E_{xcm} and E_{icm} given above and

$$\begin{aligned} P_{xcm} &= SQRT(E_{xcm}^2 - m_x^2) \\ P_{icm} &= SQRT(E_{icm}^2 - M_p^2) \quad . \end{aligned}$$

Equation (2.39) gives $d\sigma/dx$ in term of integrations with respect to the production angle θ, the invariant mass of the hadronic final state M_f and the momentum transfer t. From Eq. (2.39), one can easily obtain $d\sigma/(dxd\theta)$, $d\sigma/(dxd\theta dM_f^2)$ $d\sigma/(dxd\theta dM_f^2 dt)$, etc., using the integrand. The numerical results will be discussed in Sec. 4 after we discuss the backgrounds in Sec. 3.

III. BACKGROUND CALCULATIONS

Since the X particle is produced by an electron via the process shown in Fig. 1, one of its decay modes must be $X \to e^+e^-$. The partial widths corresponding to various types of X particles decaying into e^+e^- are given by[8]

$$\Gamma_i = \frac{1}{2} m_x \alpha_x F_i(z) \quad , \tag{3.1}$$

where $z = (m_e/m_x)^2$ and

$$\begin{aligned} F_s(z) &= (1-4z)^{3/2} \\ F_{ps}(z) &= (1-4z)^{1/2} \\ F_v(z) &= \frac{2}{3}(1-4z)^{1/2}(1+2z) \\ F_{av}(z) &= \frac{2}{3}(1-4z)^{3/2} \quad . \end{aligned}$$

In the PEGASYS experiment $z \to 0$, hence

$$\Gamma_s = \Gamma_{ps} = \frac{1}{2} m_x \alpha_x \quad , \tag{3.2}$$

and

$$\Gamma_v = \Gamma_{av} = \frac{1}{3} m_x \alpha_x \quad . \tag{3.3}$$

If we ignore the decay probabilities into all other channels, we can obtain the lifetime

$$\tau_i = \hbar/\Gamma_i = 1.316 \times 10^{-24}\ s\ \mathrm{GeV}/[m_x \alpha_x F_i(z)] \quad , \tag{3.4}$$

and the decay length is

$$c\tau_i\gamma = 3.95 \times 10^{-14} cm \frac{E_x}{m_x} \frac{\mathrm{GeV}}{m_x \alpha_x F_i(z)} \quad . \tag{3.5}$$

In the PEGASYS experiment[1] we have $E_x < 14.5$ GeV and 0.1 GeV $< m_x <$ 3.5 GeV and the best available vertex detector has a spacial resolution of about 10^{-3} cm. Thus, only when $m_x \sim 0.1$ GeV and $\alpha_x < 10^{-7}$ can we observe the vertex of the decay $X \to e^+e^-$. Also, if α_x is much smaller than 10^{-7}, there will not be enough x produced. From now on we shall assume that the decay length is so small that it can be ignored. The main backgrounds are due to Figs. 3 and 4.

The contribution from Fig. 3 can be calculated easily using the result for a vector particle production and the Kroll–Wada[14] theorem. Let the invariant mass of the e^+e^- pair in Fig. 3 be the square root of $s = (P_+ + P_-)^2$. Then the cross section for producing such a pair can be obtained from the cross section for producing a vector particle of mass $M_x = \sqrt{s}$ by a replacement

$$\alpha_x \to \frac{\alpha^2}{3\pi} \left(\frac{s - 4m_e^2}{s^2} \right) ds \approx 1.13 \times 10^{-5} \frac{dm_x}{m_x} \quad , \tag{3.6}$$

where dm_x is determined by the mass resolution of the apparatus. Now we are looking for a bump due to production of an x particle whose intrinsic width is negligible. The background is a smooth curve given by (3.6); only the statistical fluctuation will give a bump-like look. Let us assume that there are N events in the interval ds due to the background. The statistical fluctuation will be $\sqrt{N}$. Let the background cross section be σ and its statistical fluctuation be $d\sigma$. Then $d\sigma/\sigma = \sqrt{N}/N$; thus $d\sigma = \sigma/\sqrt{N}$. In other words, the more meaningful background to the problem is less serious than the number obtained from Eq. (3.6); it should be multiplied by $1/\sqrt{N}$.

The backgrounds due to Fig. 4 can be calculated exactly. We give here a simpler treatment using Weissäcker–Williams method. First let us point out that the signal-to-background ratio can be considerably improved by detecting the outgoing electron P_2 as well as the pair from the decay of the X particle. They should be arranged such that neither $\vec{k}$ or $\vec{P_2}$ is in the forward angle but the sum of their transverse momenta is nearly zero. In general, even if only the pair from the decay of x are detected, the outgoing P_2 will prefer to go in the above-mentioned symmetric direction because this is where the minimum momentum transfer to the target occurs. Comparing Figs. 1 and 4, the momentum transfer to the target labeled q in the two cases are identical. In Fig. 4, the outgoing electron P_2 will prefer to go to the forward angle instead of the symmetric angle because the photon propagator labeled k_1 in Fig. 4 can become almost on the mass shell when P_2 is in the forward direction. Let us therefore calculate the background contribution due to Fig. 4, with the above geometry in mind.

1. The equivalent photon flux of the electron[11] is

$$\rho_e(k_1,t')dk_1dt' = \frac{\alpha}{\pi}\frac{dk_1}{k_1}\left[\frac{1+(1-x)^2}{2}\frac{1}{t'} - \frac{m_e^2x^2}{t'^2}\right]dt' \tag{3.7}$$

$$\approx \frac{2\alpha}{\pi}\frac{dx}{x}\frac{1+(1-x)^2}{2}\frac{d\theta_2}{\theta_2} \quad , \tag{3.8}$$

where $k_1 = E_1 - E_2$ is the energy of the photon, $t' = -(P_1 - P_2)^2 \approx E_1E_2\theta_2^2$ and $x = k_1/E_1$.

Integrating (3.7) with respect to t', we obtain the more familiar expression for the equivalent photon flux when P_2 is left undetected:

$$\int_{t_{min}}^{t_{max}} \rho_e(k_1, t')dt' = \frac{\alpha}{\pi}\frac{dk_1}{k_1}\left[\frac{1+(1-x)^2}{2}\ell n\frac{t_{max}}{t_{min}} - (1-x)\right] \quad , \tag{3.9}$$

where $t_{min} = m_e^2 x^2(1-x)$ and $t_{max} = 4E_1E_2$.

For $E_1 = 14.5$ GeV, $x \sim 1$, the ratio of Eq. (3.9) to Eq. (3.8) is $(\theta_2/\Delta\theta_2)\ell n$ $(2E_1/m_e) = 11\theta_2/\Delta\theta_2$, which shows that the background can be reduced by two orders of magnitude if $\theta_2/\Delta\theta_2 \approx 10$.

2. We ignore the facts that the two γ's in the reaction $\gamma + \gamma \to e^+e^-$ are off the mass shell, and use the mass shell cross section

$$\sigma(\gamma\gamma \to e^+e^-) \approx \frac{2\pi\alpha^2}{s} \quad , \tag{3.10}$$

where $s = (P_+ + P_-)^2$. Since we are calculating the background we set $s = m_x^2$.

3. Combining the equivalent photon flux of the electron given by Eq. (3.8), the $\gamma\gamma \to e^+e^-$ cross section given by (3.10) and the equivalent photon flux[11] of the target proton, we obtain

$$d(e^- + p \to e^- +' e^+e^-\text{pair} + \text{anything})$$

$$= \left(\frac{2\alpha}{\pi}\frac{dx}{x}\frac{1+(1-x)^2}{2}\frac{d\theta_2}{\theta_2}\right)\left(\frac{2\pi\alpha^2}{s}\right)\frac{\alpha}{\pi}\frac{ds}{s}\frac{1}{2m_p}\int_{M_p^2}^{M_{f\,max}^2} dM_f^2 \tag{3.11}$$

$$[(t - t_{min})W_2 + 2t'_{min}W_1]dt/t^2 \quad ,$$

where W_1 and W_2 are given by Eqs. (2.31) through (2.33), and

$$M_{fmax} = (M_p^2 + 2k_1 M_p)^{\frac{1}{2}} - \sqrt{s} \quad ,$$
$$t'_{min} = [s/(2k_1)]^2 \quad ,$$
$$t_{min} = t'_{min} + SQRT(t'_{min})(M_f^2 - M_p^2)/M_p \quad .$$

Note that dt can be changed into the acceptance of the pair in the following way: Let $k = P_+ + P_-$. Then

$$t = -(P_1 - P_2 - k)^2 = 2k \cdot (P_1 - P_2) + \ldots \tag{3.12}$$

Thus,

$$dt = -2|\overrightarrow{P_1 - P_2}|P_x d\cos\theta_{k_{12}}$$

Where $\theta_{k_{12}}$ is the angle between the two vectors $\vec{k} = \overrightarrow{P_+} + \overrightarrow{P_-}$ and $\overrightarrow{P_1 - P_2}$. Equation (3.12) tells us that for a given $\overrightarrow{P_2}$, t is minimum when $\vec{k}//\overrightarrow{P_1} - \overrightarrow{P_2}$, where most of the events will be concentrated. If k is given then t can be written as

$$t = -(P_1 - P_2 - k)^2 = 2P_2 \cdot (P_1 - k) + \ldots \tag{3.13}$$

which shows that t is minimum when $\overrightarrow{P_2}$ is parallel to the vector $(\overrightarrow{P_1 - k})$.

IV. NUMERICAL EXAMPLES

In Fig. 5(a) we give $d\sigma/dx$ defined by Eq. (2.39) for production of a spin 0 particle. The results from elastic and inelastic form factors, given by Eqs. (2.31) through (2.33), are summed in the figures. Figure 5(b) is similar to Fig. 5(a) except now we deal with production of a spin 1 particle. We assume $m_e/m_x \to 0$, so there is no difference in the cross section for production of pseudo scalar and scalar particles, and also between vector and axial vector particles. We also assume $\alpha_x = 1$. Using these curves, one can immediately obtain the minimum values of α_x necessary to discover particles of various masses. For example, suppose the integrated luminosity is $10^{40} cm^{-2}$ and we need at least 10 events to prove the existence of a particle. To produce a particle of mass $m_x = 3.5,\ 2.0,\ 1.0,\ 0.1$ GeV, the value of α_x must be at least $\alpha_x = 10^{-4},\ 3 \times 10^{-7},\ 10^{-8},\ 10^{-10}$ for spin 0, and $\alpha_x = 5 \times 10^{-5},\ 10^{-6},\ 10^{-8},\ 10^{-11}$ for spin 1 particle production. When $m_x \to 0$, the x dependence[2] of the cross section goes like $d\sigma/dx \to x$ for spin 0 particle production and $d\sigma/dx \to 1/x$ for spin 1 particle production (such as in ordinary bremsstrahlung emission). We note from Figs. 5(a) and (b) that in both spin 0 and spin 1 particle productions $d\sigma/dx$ tend to peak at $x = 1$ when $m_x \neq 0$. The peaking is more pronounced for the spin 0 case.

In Fig. 5(c) we plot the background using Eq. (3.11) integrated with respect to both θ_2 and t and setting $ds/s = 2dm_x/m_x = .02$. This gives the background of electron pairs due to Fig. 4. The background due to Fig. 3 is not included in Fig. 5(c). As mentioned in Sec. 3, the background due to Fig. 3 can be obtained by replacing α_x in Eq. (2.39) for production of a *vector* particle by an expression given by Eq. (3.6). Since we have assumed $dm_x/m_x = 0.01$ in our calculation for Fig. 5(c), the background due to Fig. 3 is equivalent to $d\sigma/dx$ given in Fig. 5(b) multiplied by 1.13×10^{-7}. Comparing Fig. 5(c) with Fig. 5(b) $\times 1.13 \times 10^{-7}$ we see that the latter is negligible, except when $m_x = 0.1$ GeV and $x \to 1$. We have assumed the mass resolution of $dm_x/m_x = 0.01$ for convenience of presenting our result. The actual value of dm_x/m_x is dependent upon E_x and m_x.

Inspection of Figs. 5(a), (b) and (c) shows that the signal-to-background ratio is greatest when x is near unity, hence high x events should be selected. At $x = .95$ the signal-to-background ratios for $m_x = 3.5,\ 2.0,\ 1.0$ and 0.1 GeV are respectively $(1.36 \times 10^2,\ 3.89 \times 10^3,\ 1.57 \times 10^4,\ 5.88 \times 10^4)$ $(\alpha_x m_x/\Delta m_x)$ for spin 0 particle production and $(3.19 \times 10^2,\ 8.80 \times 10^3,\ 3.60 \times 10^4, 1.36 \times 10^5)$ $(\alpha_x m_x/\Delta m_x)$ for spin 1 particle production.

In Figs. 6, 7 and 8 we give the energy-angle distributions of the x particle, $d\sigma/(dxd\sigma)$, for both spin 0 and spin 1 cases, and the masses $m_x = 0.1, 1.0, 2.0$ GeV, assuming again $\alpha_x = 1$. The energy-angle distributions of the background are also given in Figs. 6(c), 7(c) and 8(c), assuming $\Delta m_x/m_x = .01$. These curves are obtained by integrating (3.11) with respect to θ_2 [see Eq. (3.9)].

We observe the following characteristics of the energy-angular distributions:

1. Comparing Fig. 4 with Fig. 1, we note that the photon propagators labeled q in two cases are the same. In Fig. 1, the electron propagator makes the angular dependence more sharply peaked toward the forward angle than the background. The extra angular dependence due to the electron propagators in Fig. 1 is

$$\frac{1}{\left(\theta_k^2 + \frac{m_x^2}{E_1^2}\frac{(1-x)}{x^2}\right)^2} .$$

   This factor makes the cross sections fall off sharper with θ_k when m_x is small and x is near 1.

2. From the above analysis we see that the signal-to-background ratio is better at small angles if only the pair is detected; but as we have pointed out in the last section, tremendous increase in signal-to-background ratio can be achieved if we tag the final electron slightly off the forward angle in such a way that the momentum of the pair $\vec{k} = \overrightarrow{P_+} + \overrightarrow{P_-}$ is parallel to $\overrightarrow{P_1} - \overrightarrow{P_2}$.

We note that in this kinematical condition the final state momentum of the target $\overrightarrow{P_f}$ is parallel to $\vec{k}$ because of the momentum conservation. On the other hand, if $\overrightarrow{P_2}$ is chosen to be parallel to $\overrightarrow{P_1} - \vec{k}$, then $\overrightarrow{P_f}$ is parallel to $\overrightarrow{P_2}$.

V. DISCUSSIONS

Hawkins and Perl[9] have speculated that there might be charged-lepton specific forces. Our X particles could be the particles associated with such forces. Let us use the analogy with QCD. Similarly to the color for the quarks, we may have a leptonic "color" possessed only by leptons. This leptonic color acts as a source for a new force via exchange of a new kind of a gluon that would be the candidate for our spin 1 X particle. We do not know such a force is parity-conserving or not. This can be tested by using a polarized electron beam. The existence of the parity-violating term $\vec{\sigma} \cdot \vec{k}$, where $\vec{\sigma}$ is the electron spin and $\vec{k}$ is the momentum of the X particle in the angular distribution of the X particle will indicate parity violation. If there is a new force between leptons, we might expect some bound states to be formed by leptons and they may show up as spin 0 x particles. There may also be Higgs-like particle and pseudo-Goldstone bosons coupled only to leptons. In this paper, we do not attempt to build a detailed model of the X particles because we need to assume only two parameters α_x and m_x to perform the calculation for the cross sections.

We also cannot specify whether the coupling is flavor-dependent. This can be determined by the decay rates of X into $e^{\pm}$, μ^2 and $\tau^{\pm}$. Production of x particles using a muon beam can also shed light on this question. As long as $m_x \gg m_\mu$, we may use all the equations given by Eqs. (2.10) through (2.30). However, even if the mass of muon is not negligible compared with m_x, it is trivial to change all of our equations, because exact expressions for the cross sections can be generated by a computer using Eqs. (2.2) through (2.9).

Our x particles do not have to be coupled to leptons only. If they couple to hadrons as well leptons, the only change would be that the branching fractions to the leptons are reduced by about a factor of two, which can be obtained experimentally.

ACKNOWLEDGMENTS

The author wishes to thank Martin Perl, Eli Piasetzky, Sayed Rokni, and Karl Van Bibber for discussions on the PEGASYS Project at SLAC. The author would also like to thank Michael Riordan for carefully reading the manuscript and offereing many valuable comments. This work was supported by the Department of Energy, contract No. DE–AC03–76SF00515.

REFERENCES

1. Karl Van Bibber *et al.*, *PEGASYS Proposal at SLAC*, (1989).
2. Y. S. Tsai, Phys. Rev. **D34**, 1326 (1986).
3. E. M. Riordan *et al.*, Phys. Rev. Lett. **59**, 755 (1987).
4. A. Konaka *et al.*, Phys. Rev. Lett. **57**. 659 (1986).
5. M. Davier *et al.*, Phys. Lett. **180B**, 295 (1986).
6. C. Brown *et al.*, Phys. Rev. Lett. **57**, 2101 (1986).
7. J. Schweppe *et al.*, Phys. Rev. Lett. **51**, 2261 (1983); M. Clemente *et al.*, Phys. Lett. **B137**, 41 (1984); T. Cowan *et al.*, Phys. Rev. Lett. **54**, 1761 (1985); T. Cowan *et al.*, Phys. Rev. Lett. **56**, 444 (1986).
8. J. Reinhardt *et al.*, Phys. Rev. **C33**, 194 (1986).

9. C. A. Hawkins and M. L. Perl, SLAC–PUB–4721 (1988).

10. A. C. Hearn, *Reduce II User's Manual*, Stanford Artificial Intelligence Project Memo AIM–133 (1970).

11. Y. S. Tsai, Rev. Mod. Phys. **46**, 815 (1974).

12. W. Atwood, private communication.

13. Eli Piasetzky and Sayed Rokni have already put Eq. (2.1) into the Monte Carlo program.

14. N. Kroll and W. Wada, Phys. Rev. **98**, 1355 (1955).

FIGURE CAPTIONS

Fig. 1. Feynman diagrams for production of an x particle by an electron beam. The target particle P_i is a proton.

Fig. 2. The coordinate system used in the integration of the outgoing electron P_2. The subscript s refers to the rest frame of $U = P_2 + P_f = P_1 + P_i - k$. In this frame both k and P_1 are in the $x - z$ plane, the direction of the vector $\vec{P_1} - \vec{k}$ is chosen as the z axis and the direction of $\vec{P_i}$ is along the negative z direction.

Fig. 3. Background $e^{\pm}$ pair production due to internal conversion of the bremsstrahlung photon.

Fig. 4. Background $e^{\pm}$ pair production due to two photon annihilation.

Fig. 5. (a) $d\sigma/dx$ for production of a spin 0 particle in the reaction $e + p \to X + e+$ anything at $E_1 = 14.5$ GeV in unit of cm^2 assuming $\alpha_x = 1$. (b) The same as above for a spin 1 particle. The background due to the mechanism of Fig. 3 can be obtained by multiplying 1.13 $\times 10^{-5} \Delta m_x/m_x$ onto this graph. (c) Background due to 2γ process shown in Fig. 4. Mass resolution of $\Delta m_x/m_x =$ .01 is assumed.

Fig. 6. (a) $d\sigma/(dx d\sigma)$ for production of a spin 0 particle in the reaction $e + p \to X + e+$ anything at $E_1 = 14.5$ GeV in unit of cm^2, assuming $\alpha_x = 1$ and $m_x = 0.1$ GeV. (b) The same as above for a spin 1 particle. The background due to the mechanism of Fig. 3 can be obtained by multiplying 1.13×10^{-5} $\Delta m_x/m_x$ onto this graph. (c) Background due to 2γ process shown in Fig. 4. Mass resolution of $\Delta m_x/m_x = .01$ is assumed.

Fig. 7. Same as Fig. 6 except $m_x = 1.0$ GeV.

Fig. 8. Same as Fig. 6 except $m_x = 2.0$ GeV.

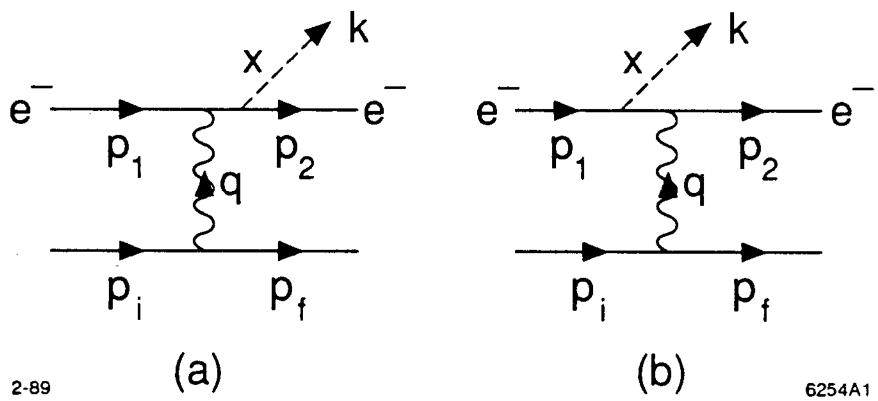

Fig. 1

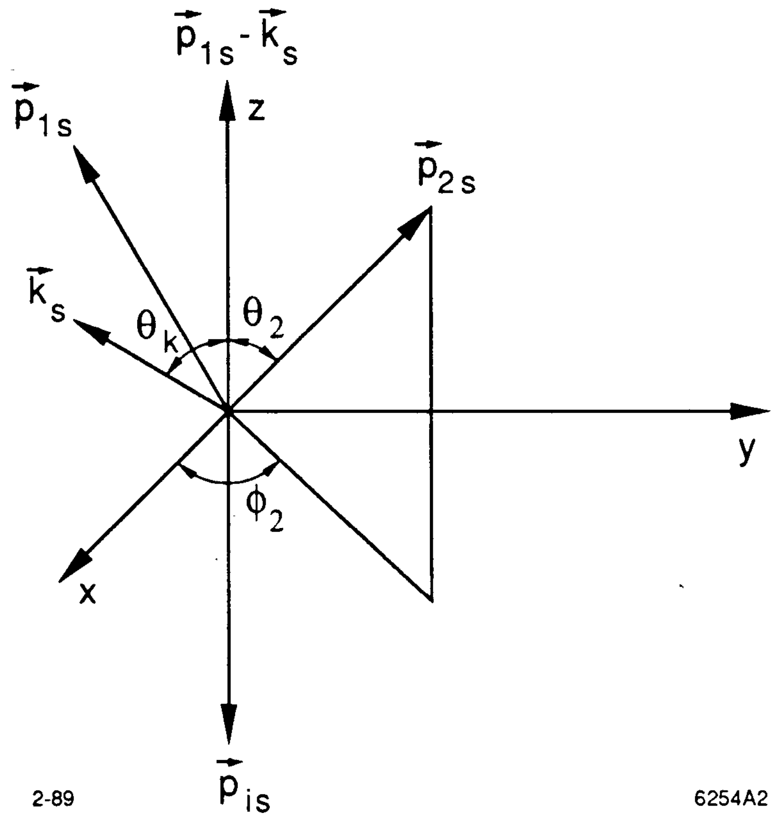

$\vec{p}_{1s}-\vec{k}_s$
z
$\vec{p}_{1s}$
$\vec{p}_{2s}$
$\vec{k}_s$
θ_k
θ_2
y
ϕ_2
x
$\vec{p}_{is}$
2-89
6254A2

Fig. 2

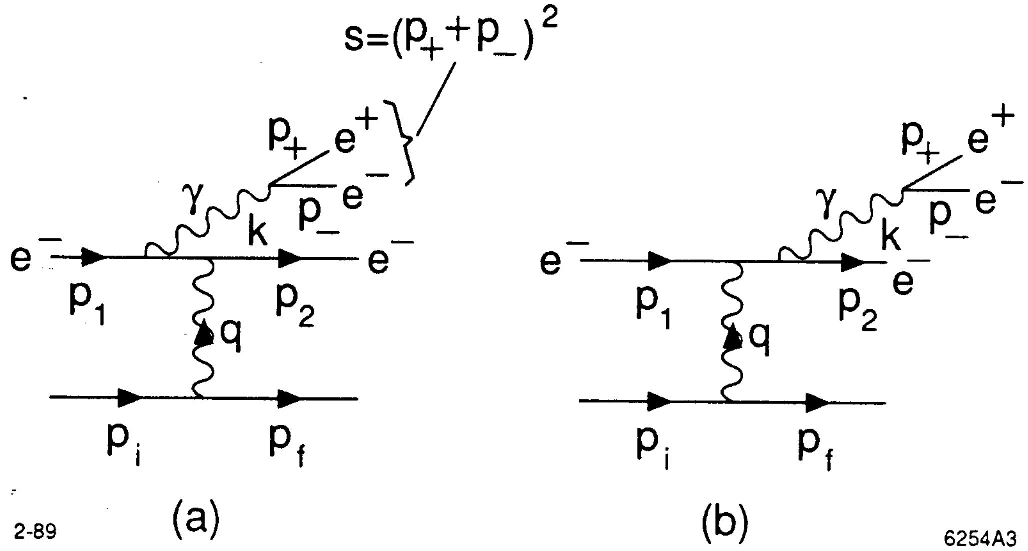

Fig. 3

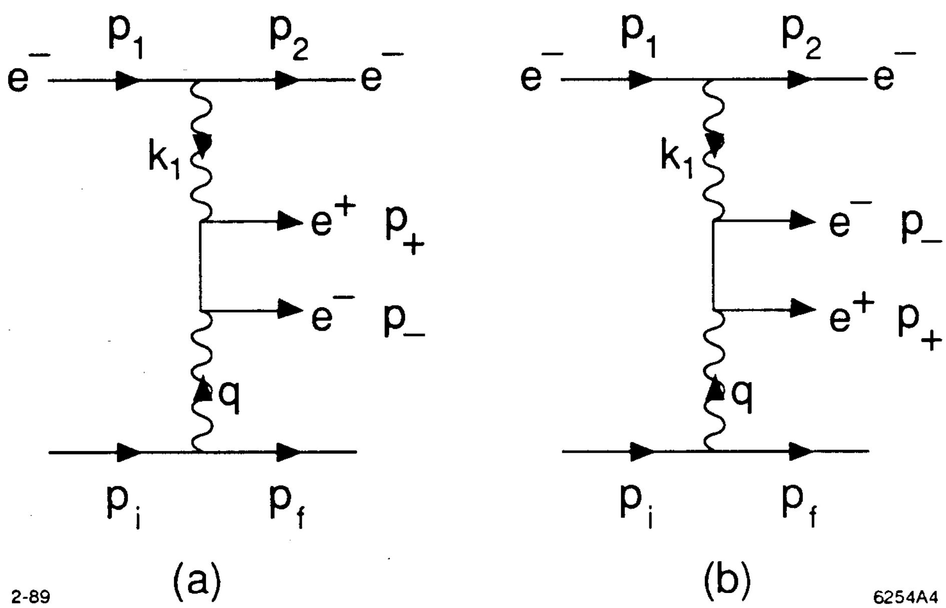

Fig. 4

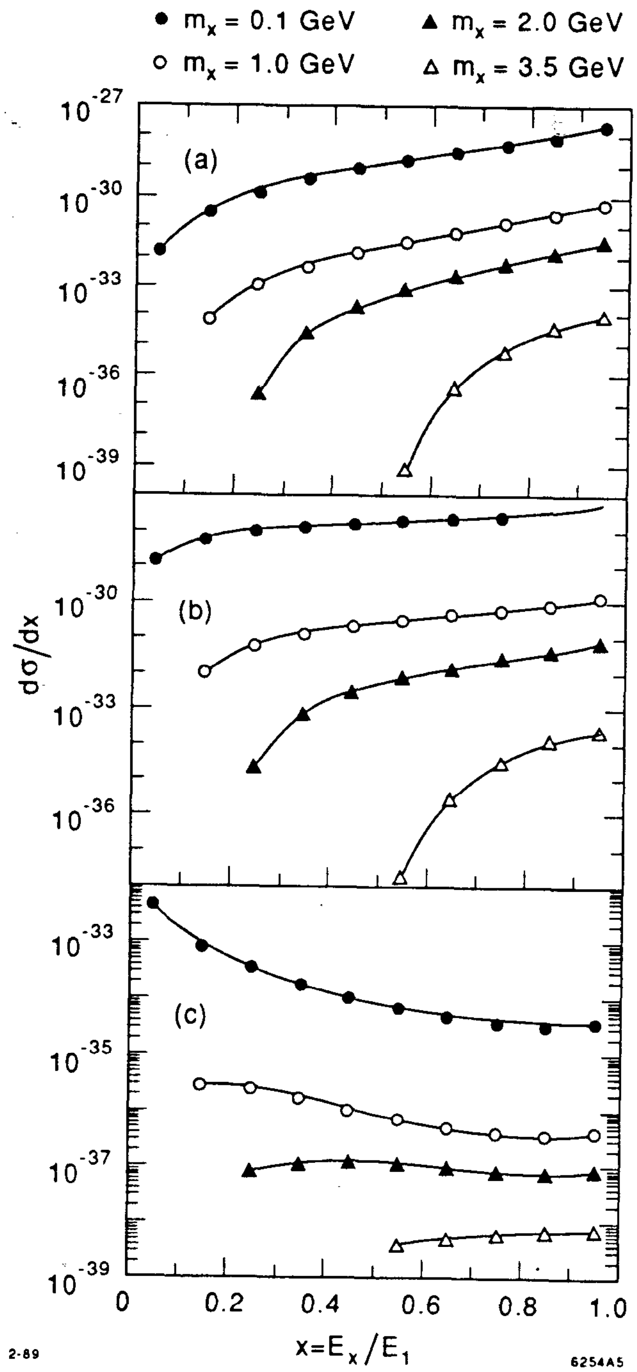

● m_x = 0.1 GeV
▲ m_x = 2.0 GeV
○ m_x = 1.0 GeV
△ m_x = 3.5 GeV
(a)
(b)
(c)
10^{-27}
10^{-30}
10^{-33}
10^{-36}
10^{-39}
10^{-35}
10^{-37}
$d\sigma/dx$
0
0.2
0.4
0.6
0.8
1.0
$x=E_x/E_1$
2-89
6254A5

Fig. 5

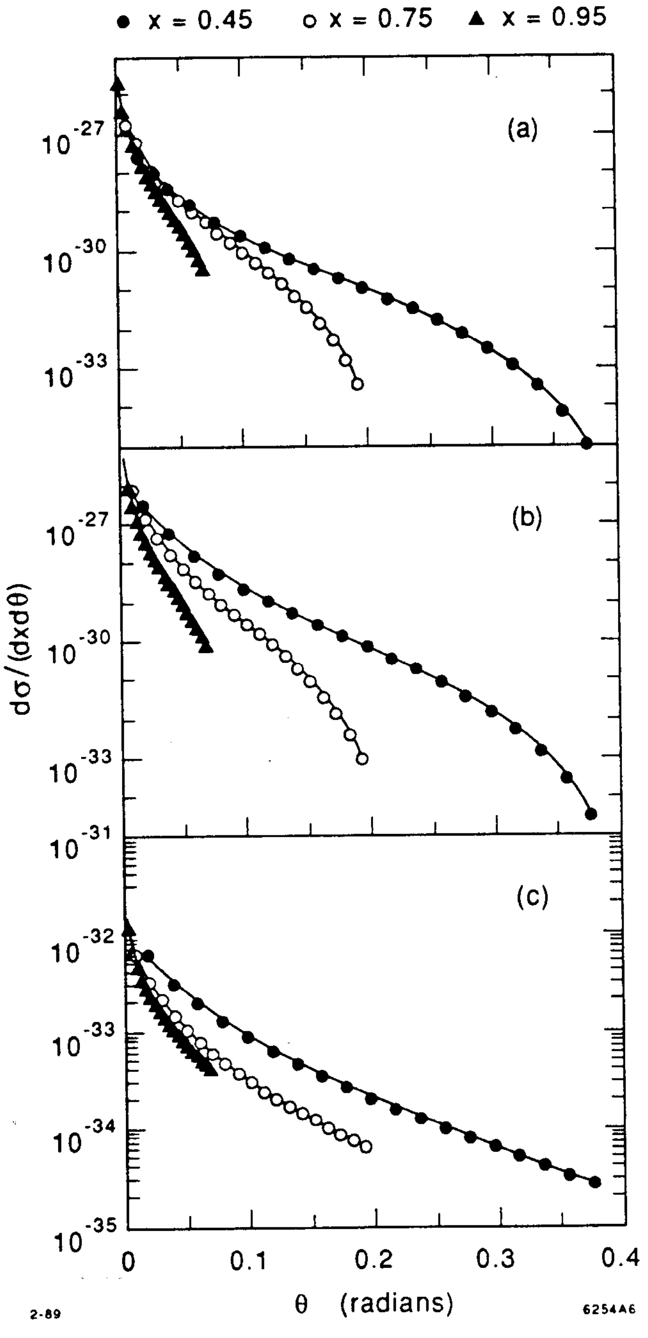

● x = 0.45 ○ x = 0.75 ▲ x = 0.95
(a)
(b)
(c)
$d\sigma/(dx d\theta)$
10^{-27}
10^{-30}
10^{-33}
10^{-31}
10^{-32}
10^{-34}
10^{-35}
0
0.1
0.2
0.3
0.4
θ (radians)
2-89
6254A6

Fig. 6

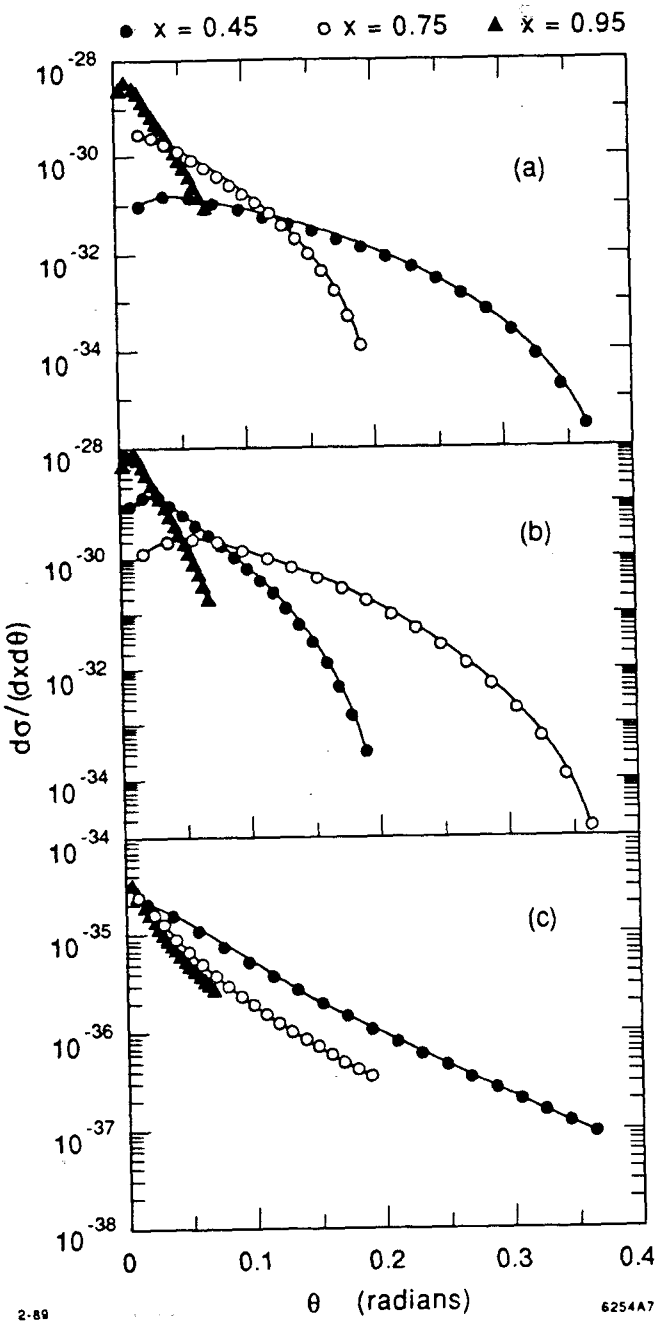
● x = 0.45 ○ x = 0.75 ▲ x = 0.95
(a)
(b)
(c)
$d\sigma/(dx d\theta)$
10^{-28}
10^{-30}
10^{-32}
10^{-34}
10^{-35}
10^{-36}
10^{-37}
10^{-38}
0
0.1
0.2
0.3
0.4
θ (radians)
2-89
6254A7

Fig. 7

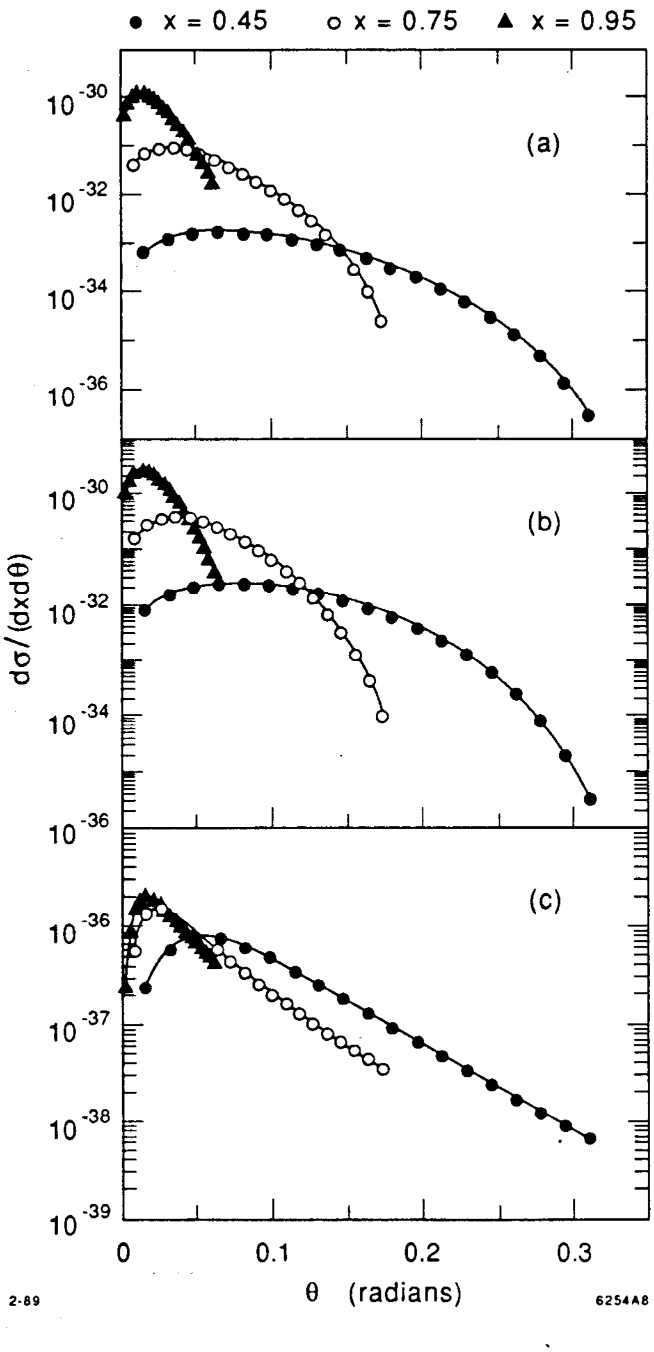

Fig. 8